Journal of Rock Mechanics and Geotechnical Engineering 6 (2014) 477–485

Contents lists available at ScienceDirect

Journal of Rock Mechanics and Geotechnical Engineering

journal homepage: www.rockgeotech.org

Full length article

Influence of soil–structure interaction on seismic collapse resistance of super-tall buildings

Mengke Li [a], Xiao Lu [b], Xinzheng Lu [a,*], Lieping Ye [a]

[a] Key Laboratory of Civil Engineering Safety and Durability of Education Ministry, Tsinghua University, Beijing 100084, China
[b] School of Civil Engineering, Beijing Jiaotong University, Beijing 100044, China

ARTICLE INFO

Article history:
Received 23 January 2014
Received in revised form
5 April 2014
Accepted 17 April 2014
Available online 24 June 2014

Keywords:
Soil–structure interaction
Substructure
Super-tall building
Collapse resistance
Numerical simulation

ABSTRACT

Numerous field tests indicate that the soil–structure interaction (SSI) has a significant impact on the dynamic characteristics of super-tall buildings, which may lead to unexpected structural seismic responses and/or failure. Taking the Shanghai Tower with a total height of 632 m as the research object, the substructure approach is used to simulate the SSI effect on the seismic responses of Shanghai Tower. The refined finite element (FE) model of the superstructure of Shanghai Tower and the simplified analytical model of the foundation and adjacent soil are established. Subsequently, the collapse process of Shanghai Tower taking into account the SSI is predicted, as well as its final collapse mechanism. The influences of the SSI on the collapse resistance capacity and failure sequences are discussed. The results indicate that, when considering the SSI, the fundamental period of Shanghai Tower has been extended significantly, and the collapse margin ratio has been improved, with a corresponding decrease of the seismic demand. In addition, the SSI has some impact on the failure sequences of Shanghai Tower subjected to extreme earthquakes, but a negligible impact on the final failure modes.

1. Introduction

With the rapid economic development in China over the past several decades, China has entered a period in which the design and construction of super-tall buildings are proceeding at an extremely rapid pace. Statistics (Li, 2011) indicate that more than 350 super-tall buildings higher than 200 m have been built in China till 2010, such as the China World Trade Center Tower III (330 m), the Shanghai World Financial Center (492 m) and the Shanghai Jin Mao Tower (421 m). In addition, a series of super-tall buildings, e.g. Ping An Tower (660 m), Shanghai Tower (632 m) and Tianjin Goldin 117 Mega Tower (597 m), are under construction. Because super-tall buildings have a major impact on the economy and society and most are constructed as the landmarks of a city, the seismic safety of these super-tall buildings is a critically important issue. Such buildings basically have complex structural systems and adopt novel mega-structural components. Consequently, the structural performance and design philosophy of super-tall buildings remain immature and thus further studied are needed.

Generally, conventional seismic design and analysis practice do not take into account the flexibility of the foundation and adjacent soil. The foundation and the superstructure are typically designed as two independent systems, and the superstructure is constrained at the bottom. As a consequence, the evaluated seismic performance of the building only depends on the superstructure. This method is simple and convenient, but the dynamic characteristics and seismic performances of buildings without considering the flexibility of the foundation and adjacent soil may be significantly different from those of the actual buildings, which may lead to an unsafe design (Mylonakis and Gazetas, 2000), especially for the seismic design and analysis of important structures, such as super-tall buildings.

To identify the effect of the soil–structure interaction (SSI) on the dynamic characteristics of super-tall buildings, many researchers have conducted a number of field tests, laboratory tests and numerical simulations. Some typical comparisons on the field test period, laboratory test period and calculation period of super-tall buildings are shown in Table 1. Theoretically, because most of the numerical models used to calculate the structural period do not consider the contribution of non-structural components to the

* Corresponding author. Tel.: +86 10 62795364.
E-mail address: luxz@tsinghua.edu.cn (X. Lu).

http://dx.doi.org/10.1016/j.jrmge.2014.04.006

Table 1
Typical comparison of field test period, laboratory test period and numerical simulation period.

Building	Height (m)	Field test period (s)		Laboratory test period (s)		δ_1 (%)		Numerical simulation period (s)		δ_2 (%)	
		T_1	T_2	T_1	T_2	T_1	T_2	T_1	T_2	T_1	T_2
Shanghai World Financial Center (Zhu et al., 2005; Zhu and Lu, 2006; Lu et al., 2009)	492	6.502	6.398	5.542	5.542	−14.76	−21.74	6.5	5.8	−0.03	−9.35
Shanghai Triumphal Arch Building (Lu et al., 2001)	100	1.795	1.383	1.577	1.082	−12.14	−21.76				
Shanghai Jin Mao Tower (Li, 2007)	420.5	6.862	6.829					5.637	5.679	−17.85	−16.84
Canton Tower (Wang et al., 2007; Chen et al., 2012)	610	10.68	7.191					9.703	6.714	−9.15	−6.63

Note: T_1 and T_2 represent the first two translational vibration periods of the building, respectively. The relative deviations δ_1 and δ_2 respectively indicate the differences of laboratory test period and numerical simulation period from field test period.

overall structural stiffness, the field test period would be shorter than the calculation period. This phenomenon is also very common in multi-story structures (Gao and Bu, 1993). However, it is clearly demonstrated in Table 1 that the first two translational natural vibration periods measured in the field tests of super-tall buildings are all longer than those calculated from laboratory tests or numerical simulations and the maximum relative deviation reaches approximately 21%. The main reason for this discrepancy is that the laboratory test models or the analytical models constrain the superstructure at the bottom without considering the flexibility of the foundation and adjacent soil, which overestimates the stiffness of the entire system. Therefore, the influence of the SSI on the seismic performance of super-tall buildings cannot be ignored.

Extensive studies have shown the critical role of the SSI in the seismic responses of structures (Veletsos and Meek, 1974; Wolf, 1985; Ciampoli and Pinto, 1995; Gazetas and Mylonakis, 1998; Stewart et al., 1999; ATC, 2012). It is becoming widely accepted that the seismic design and analysis of structures should take the SSI effect into consideration. Laboratory test and numerical simulation are two major tools for understanding the behavior of the entire structure–foundation–soil system. Some researchers have conducted experimental studies to investigate the SSI effect. For example, Luco et al. (1988) performed forced vibration field tests for a 9-story reinforced concrete building, namely the Millikan Library Building, to study the SSI effect. The tests indicated that the SSI had a significant effect on the dynamic properties of the building and the rigid-body motion caused by the translation and rocking of the base accounted for over 30% of the total response on the roof. Chang et al. (2007) performed dynamic centrifuge model tests of frame–wall–foundation structural systems to investigate their seismic performance and energy dissipation. Lu et al. (2000) conducted shaking table tests on a dynamic soil–structure system to study the seismic response of the dynamic SSI system. The results indicated that the natural vibration period of the system in soft soil conditions was significantly larger than that in the rigid base condition, and the damping ratio of the system was larger than that of the superstructure. The ground motion at the foundation was different from that of the free field because of the vibrational feedback from the superstructure. The acceleration response at the top of the superstructure was dominated by the rotation of the basement and adjacent soil, followed by the translational movement. In addition, Deng et al. (2012), Drosos et al. (2012) and Liu et al. (2012) studied the nonlinear SSI effect using centrifuge model tests or shaking table tests. Ravichandran et al. (2012), Wang (2012) and Banerjee and Lee (2013) studied the seismic performance of the pile foundation and soil–pile interaction by conducting a series of centrifuge model tests.

With the continuous development of computer science, numerical methods have also become important tools for SSI research. For example, Chaallal and Ghlamallah (1996) analyzed the seismic performance of 20-story ductile coupled-shear-wall models that considered the SSI effect. The study indicated that the consideration of foundation flexibility elongated the fundamental period by up to 33% and amplified the deflections by up to 81%; however, the stresses in the walls and coupling beams decreased, particularly in the lower stories. The SSI had no obvious effect on the rotational ductility demands of the coupling beams. Mylonakis et al. (2006) investigated the role of the SSI in the collapse of the elevated Hanshin Expressway during the 1995 Kobe earthquake. Han (2002) studied the seismic behavior of a 20-story frame tall building by considering the soil–pile interaction, leading to the conclusion that the rigid base model overestimated the stiffness and underestimated the damping. Lu et al. (2003) performed a three-dimensional (3D) finite element (FE) analysis on the dynamic SSI of a 12-story frame structure using the FE program ANSYS and discussed the influence of various parameters, such as soil property, structural stiffness and buried depth, on the seismic response of the SSI system. Farghaly and Ahmed (2013) performed a 3D time-history analysis of structure–foundation–soil system models under strong earthquake ground motion and concluded that the SSI could have a detrimental effect on the building performance. Although great progress has been made in the studies of the SSI, the superstructures on which most studies focused are mainly multi-story buildings and bridges. There are few studies examining the SSI effect on the seismic performance of super-tall buildings. Jiang et al. (2013) took the Shanghai Tower as the research object and discussed the influence of the SSI on the dynamic properties and seismic displacement responses. The results indicated that the consideration of the pile–soil–structure interaction elongated the vibration period and amplified the roof deflection. In contrast, the inter-story drift ratio was smaller than that of the rigid base model. In addition, the studies mentioned above were mainly focused on the SSI effect on the structural dynamic properties and seismic performance, such as the displacement and the internal force response of the superstructures. Studies investigating the role of the SSI effect on the collapse resistance and collapse mechanism of the superstructure have been rarely reported in the literature.

Therefore, taking a typical super-tall building, the Shanghai Tower with a total height of 632 m, as the research object, the substructure approach is adopted to simulate the SSI effect on the seismic responses of the building. The refined FE model of the superstructure of the Shanghai Tower and the simplified analytical model of the foundation and adjacent soil are established. The collapse process of the Shanghai Tower with the SSI effect is predicted, and the influence of the SSI on the collapse mechanism and the collapse resistance capacity are discussed.

2. Finite element model of Shanghai Tower and its soil–foundation system

The SSI is a very complex nonlinear process and these nonlinearities may include: (1) yielding of the lateral resistance system in the superstructure; (2) yielding of the soil; (3) gapping between the foundation and the soil; and (4) yielding of the foundation structural elements. Considering all these issues in the response history analysis is a formidable task, even with modern computational capabilities. The numerical methods used to evaluate the SSI effect can be categorized as the direct analysis approach and the substructure approach (ATC, 2012). In the direct analysis approach, the soil, foundation and structure are included within the same model and analyzed as a complete system, as schematically depicted in Fig. 1a. The direct analysis approach can address the detailed response and damage to the superstructure, foundation and soil when subjected to earthquakes. However, this method is difficult to be implemented, because of the large computational workload, especially for complex structures. Another method is the substructure approach (Pitilakis and Clouteau, 2010), in which a series of springs are incorporated to represent the foundation and adjacent soil, as depicted in Fig. 1b. In 1953, Meyerhof (1953) used the equivalent stiffness method to consider the interaction between the frame structure and the soil. According to different research objectives, the substructure approach can also be classified into two subclasses: (1) nonlinear structure and equivalent-linear soil; and (2) nonlinear soil and linear structure. Structural engineers focus more attention on the responses of the superstructure than the soil. Hence, they generally choose the nonlinear structure and equivalent-linear soil model (Mylonakis and Gazetas, 2000; Avilés and Pérez-Rocha, 2003; Jarernprasert et al., 2013) to evaluate the structural seismic responses.

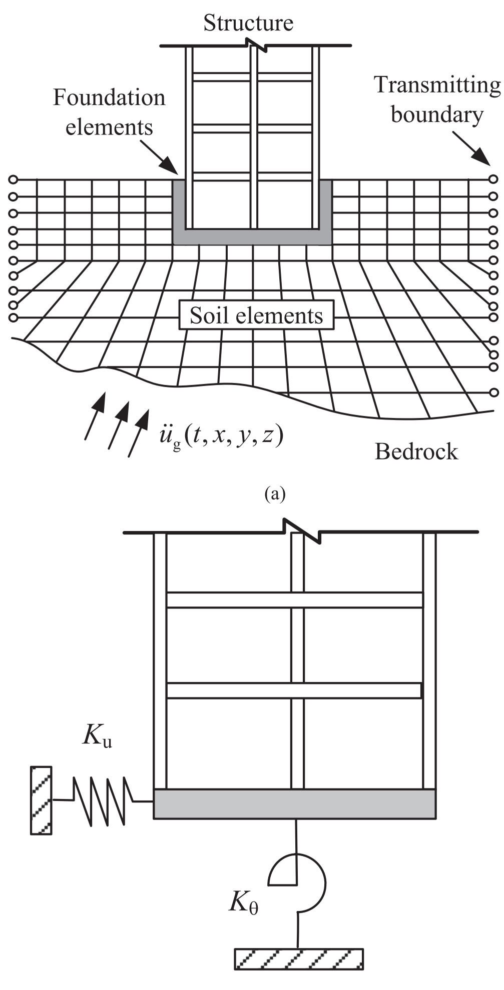

Fig. 1. Schematic illustration of analytical methods of the SSI. (a) Direct analysis approach; and (b) Substructure approach.

Note that in this study, the Shanghai Tower has hundreds of thousands of different components. The direct analysis approach, in which the 3D refined FE model of the superstructure of the Shanghai Tower, its foundation and adjacent soil must be established, will lead to a substantial volume of computation, making it difficult to perform a study on the parameter sensitivity. In addition, this study focuses on the seismic response and collapse resistance of the superstructure of the Shanghai Tower, rather than the seismic response of only the foundation and soil. For the above reasons, the substructure approach including the nonlinear structure and equivalent-linear soil is adopted to evaluate the seismic responses of the Shanghai Tower, in which a series of springs are incorporated to represent the foundation and adjacent soil.

The shaking table test of a soil–structure system conducted by Lu et al. (2000) indicated that the seismic responses of the superstructure were dominated by the rotation of the basement and adjacent soil, followed by the translational movement. Because the total height of the Shanghai Tower is much greater than the embedded depth of its foundation, this research will focus on the influence of the rotation of the soil–foundation system on the seismic responses of superstructure subjected to a lateral earthquake; thus, the horizontal and vertical movements of the soil–foundation system are correspondingly ignored. Therefore, the soil–foundation system of the Shanghai Tower is simplified as a series of linear rotation springs at the bottom of the building, and the main parameters of the springs are calibrated by the refined FE model of the soil–foundation system. The details of the superstructure of the Shanghai Tower and the soil–foundation system are presented in the following sections.

2.1. Overview and finite element model of the Shanghai Tower

The Shanghai Tower is a multi-purpose office building located in Lujiazui, Shanghai, China. The tower consists of a 124-story main tower, a 7-story podium and a 5-story basement, and the total height of the tower is approximately 632 m. The mega-column/core-tube/outrigger lateral-force-resisting system is adopted for the main tower, as shown in Fig. 2 (Lu et al., 2011). According to the architectural and functional requirements, the mechanical and refuge stories divide the main tower into 8 zones along the height. The mega-column system contains 8 mega-columns extending

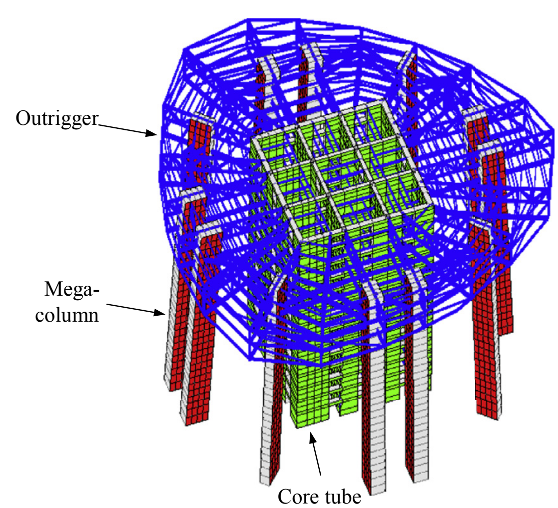

Fig. 2. Schematic illustration of the lateral-force-resisting system of the Shanghai Tower (Lu et al., 2011).

from the bottom to the top of the building and 4 corner mega-columns ending at Zone 5. All of the mega-columns are constructed using shaped-steel reinforced concrete columns, and the maximum cross-section is approximately 5300 mm × 3700 mm. The core tube is made up of a 30 m × 30 m reinforced concrete tube, and the thickness of the concrete wall decreases gradually from the bottom to the top. The outrigger system is located at the mechanical and refuge stories, i.e. the junction of each of the two zones, consisting of the circle trusses and the outriggers with a total height of 9.9 m.

The 3D FE model of the Shanghai Tower is built up based on the general FE program MSC.Marc. The diagram of the FE model is shown in Fig. 3 (Lu et al., 2011). The widely used fiber beam element model is adopted to simulate the steel frame, outrigger and steel tower at the top. The multi-layer shell element, which has outstanding nonlinear performance, is used to simulate the shear wall and coupling beam in the core tube. Meanwhile, the concentrated reinforcement, i.e. H-shaped steel, in the boundary zones of the shear wall is simulated using beam elements, which are incorporated into the shell model with sharing nodes. The combined simplified model including the multi-layer shell element and the truss element is adopted to simulate the mega-columns. The details of the modeling issues are presented in Lu et al. (2011).

2.2. Finite element model and rotational stiffness of the soil–foundation system

In substructure approach, the foundation and adjacent soil are simplified into a series of springs to consider the SSI effect. In this section, the refined FE model of the foundation and adjacent soil is established to calibrate a reasonable range of the stiffness of the rotation spring.

The schematic diagram of the foundation of the Shanghai Tower and the adjacent soil is shown in Fig. 4. The piled raft foundation, including the basement, raft and piles, is used to support its main

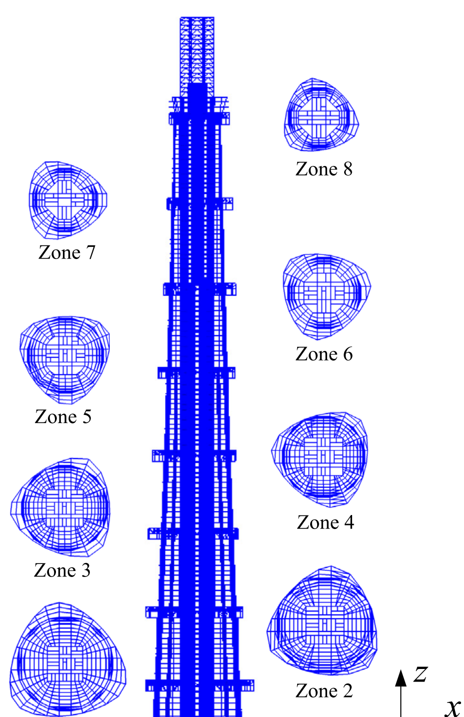

Fig. 3. 3D FE model of the Shanghai Tower (Lu et al., 2011).

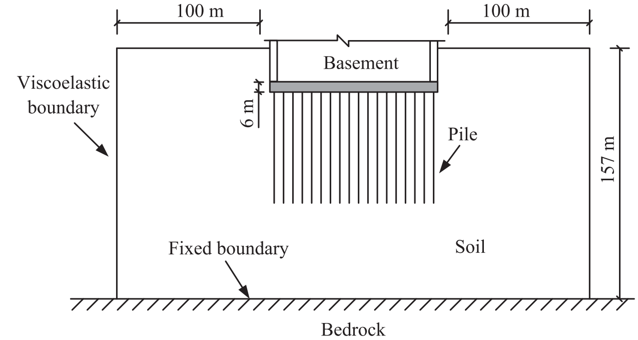

Fig. 4. Schematic diagram of the soil–foundation system of the Shanghai Tower.

tower. The planar shape of the piled raft foundation is an octagon, with a total area of 8250 m^2. The basement has 5 underground stories. The raft is constructed of reinforced concrete with a total thickness of 6 m. The top elevation of the raft is −25.4 m. The pile system is composed of a series of bored piles, each with a diameter of 1 m and a total length of approximately 87 m, and the piles are spaced at 3 m intervals in both directions. In the FE model, the piles are merged according to the assumption that the merged piles system has a stiffness approximately equal to the actual pile system. The diameter of the merged pile is 1.8 m, with the pile spacing increasing to 9 m. The material parameters of the piles remained unchanged. Jiang et al. (2013) divided the soil below the Shanghai Tower basement into approximately 4 layers and the thickness and material properties of each soil layer are described in Table 2, which are simplified from the actual conditions of the soil on site in the geological investigation report of the Shanghai Tower. In the FE model, the width of the soil at each side of the raft is 100 m. A viscoelastic boundary condition is used for the outer edge of the soil, and a fixed boundary is applied to the top face of the bedrock.

The refined FE model of the foundation and adjacent soil is implemented in the commercial software ANSYS. In this model, the slab and the wall of the basement are simulated by a shell element (Shell 63) the piles are simulated by a beam element (Beam 4) and the concrete raft is simulated by a solid element (Solid 45). The adjacent soil is also simulated by a solid element (Solid 45), and the deformation compatibility and force equilibrium at the interface of the soil and piles are achieved using shared nodes. In addition, all the material properties of the soil are treated as linear.

To obtain the linear rotational stiffness of the soil–foundation system, two forces with the same magnitude and in opposite directions are applied to the two sides of the raft. The rotational moment M can be obtained by the force at each side of the raft, F, multiplied by the length of the raft, L. Because the basement is constructed of reinforced concrete and the Young's modulus of concrete is much larger than that of the soil (as shown in Table 2), the deflection of the basement and the raft can be ignored, and the substructure rocks are considered as a rigid body under the external rotational moment M. The rotation angle θ can be determined by the relative vertical displacement on both sides of the raft

Table 2
Thickness and material properties of each soil layer in the FE model of the soil–foundation system.

Soil layer	Range of depth (m)	Specific weight (kN/m^3)	Poisson's ratio	Elasticity modulus (MPa)
1	0 to −15	18.4	0.49	20.36
2	−15 to −30	18.15	0.47	20.55
3	−30 to −115	23.8	0.46	74.4
4	−115 to −157	42.8	0.46	97.6

Table 3
Comparison of the first three translational vibration periods of the Shanghai Tower in the x and y directions.

Direction	Translational mode no.	Translational vibration period T (s)				Relative deviation δ (%)		
		Model O	Model A	Model B	Model C	Model A	Model B	Model C
x	1st	9.83	13.49	11.79	10.85	37.3	20	10.4
	2nd	3.57	3.76	3.70	3.65	5.4	3.6	2.2
	3rd	1.67	1.78	1.74	1.72	6	4.1	2.5
y	1st	9.77	13.45	11.74	10.79	37.7	20.2	10.5
	2nd	3.52	3.71	3.64	3.59	5.5	3.6	2.2
	3rd	1.66	1.76	1.73	1.70	6.3	4.3	2.6

Note: The relative deviation δ indicates the difference from Model O.

Δ divided by the length of the raft L, that is, $\theta = \Delta/L$. Consequently, the elastic rotational stiffness can be expressed by

$$K = \frac{FL^2}{\Delta} \tag{1}$$

Using the above calculation process, the equivalent rotational stiffness, K, of the soil–foundation system is determined to be approximately 4.36×10^{13} N m/rad. The factors that may influence the rotational stiffness of the soil–foundation system are very complex. For example, the adjacent soil may enter the nonlinear stage under strong earthquakes, with a corresponding change in soil stiffness. The estimated rotational stiffness of 4.36×10^{13} N m/rad may not precisely agree with the actual rotational stiffness. To account for this difference, the rotational stiffness is adjusted by 0.5 and 2.0, which yielded a range between the values of $0.5K = 2.18 \times 10^{13}$ N m/rad and $2.0K = 8.72 \times 10^{13}$ N m/rad, respectively, to assess the sensitivity of soil–foundation system to the rotational stiffness.

3. Collapse process and mechanism analysis

Based on the above analyses, three values of rotational spring stiffness representing different conditions of the soil–foundation system are obtained. For simplicity, the Shanghai Tower models, whose rotational spring stiffnesses are $0.5K$, $1.0K$ and $2.0K$, are referred to as Models A, B and C, respectively. In addition, the model with the rigid base condition is referred to as Model O.

3.1. Comparison of the basic dynamic properties

Modal analysis of the above four models is conducted using the Lanczos method. The first three translational vibration periods in the x and y directions are compared in Table 3. The fundamental periods of Model O, which does not consider the SSI effect, are 9.83 s in the x direction and 9.77 s in the y direction. All of the periods of Models A, B and C are longer than that of Model O. The comparison also indicates that the smaller the equivalent rotational spring stiffness is, the larger the fundamental period elongates. For the first translational vibration period of Models A and O, the relative deviation exceeds 30%; while for the higher vibration periods, the relative deviation becomes smaller, e.g. a 6% relative deviation for the third translational vibration period between Models A and O is a typical case. Therefore, the SSI has a significant impact on the lower order vibration mode periods, especially on the fundamental period.

To evaluate the SSI effect on the modal shapes of the Shanghai Tower, the normalized modal difference (*NMD*) (Waters, 1995) is used to identify the correlations between the translational modal shape vectors of Models A, B or C and that of Model O. The formula of *NMD* is defined as follows:

$$NMD\left(\phi_i^{\mathrm{X}}\phi_i^{\mathrm{O}}\right) = \sqrt{\frac{1 - MAC\left(\phi_i^{\mathrm{X}}\phi_i^{\mathrm{O}}\right)}{MAC\left(\phi_i^{\mathrm{X}}\phi_i^{\mathrm{O}}\right)}} \tag{2}$$

$$MAC\left(\phi_i^{\mathrm{X}}\phi_i^{\mathrm{O}}\right) = \frac{\left(\left\{\phi_i^{\mathrm{X}}\right\}^{\mathrm{T}}\left\{\phi_i^{\mathrm{O}}\right\}\right)^2}{\left(\left\{\phi_i^{\mathrm{X}}\right\}^{\mathrm{T}}\left\{\phi_i^{\mathrm{X}}\right\}\right)\left(\left\{\phi_i^{\mathrm{O}}\right\}^{\mathrm{T}}\left\{\phi_i^{\mathrm{O}}\right\}\right)} \tag{3}$$

where X represents Models A, B or C; ϕ_i^{X} and ϕ_i^{O} are the i-th modal shape vectors of Models X and O, respectively. The *MAC* is a

Table 4
Comparison between the translational vibration modes of Models A, B and C and Model O.

Translational mode no.	$NMD(\phi_i^{\mathrm{A}}\phi_i^{\mathrm{O}})$(%)		$NMD(\phi_i^{\mathrm{B}}\phi_i^{\mathrm{O}})$(%)		$NMD(\phi_i^{\mathrm{C}}\phi_i^{\mathrm{O}})$(%)	
	x direction	y direction	x direction	y direction	x direction	y direction
1st	7.67	7.68	5.05	5.07	3	3.01
2nd	11.4	11.21	7.59	7.5	4.54	4.5
3rd	10	10.31	6.83	7.08	4.18	4.34

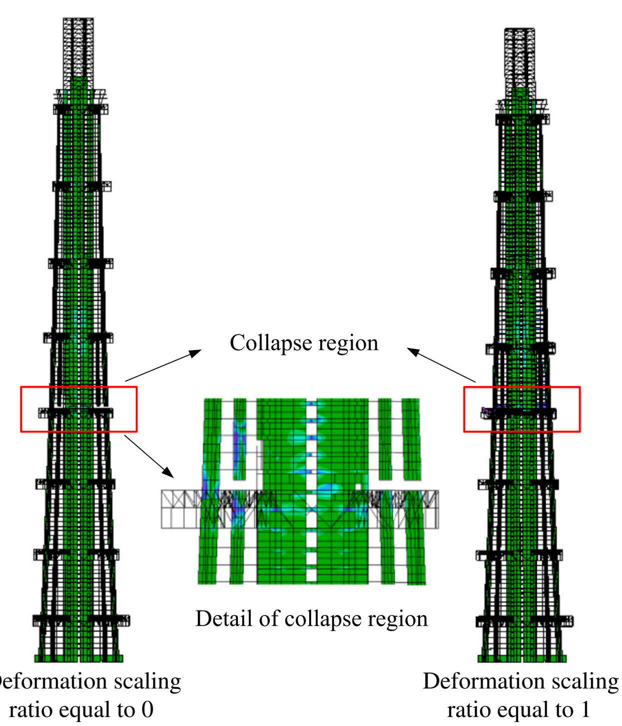

Fig. 5. Final collapse mode of Model B subjected to El-Centro in the x direction ($PGA = 1.7g$).

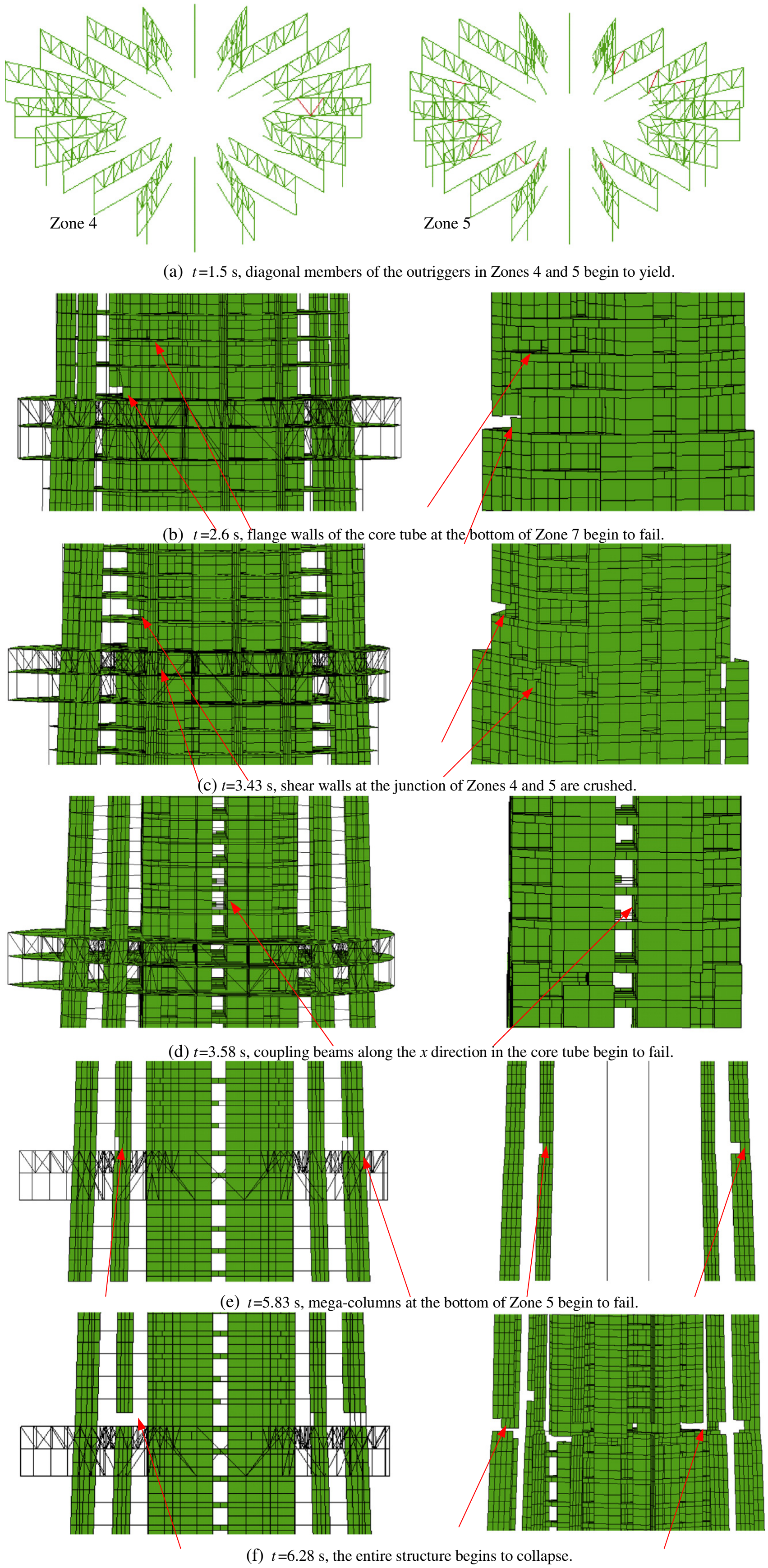

Fig. 6. Collapse process of Model B subjected to El-Centro in the x direction (PGA = 1.7g).

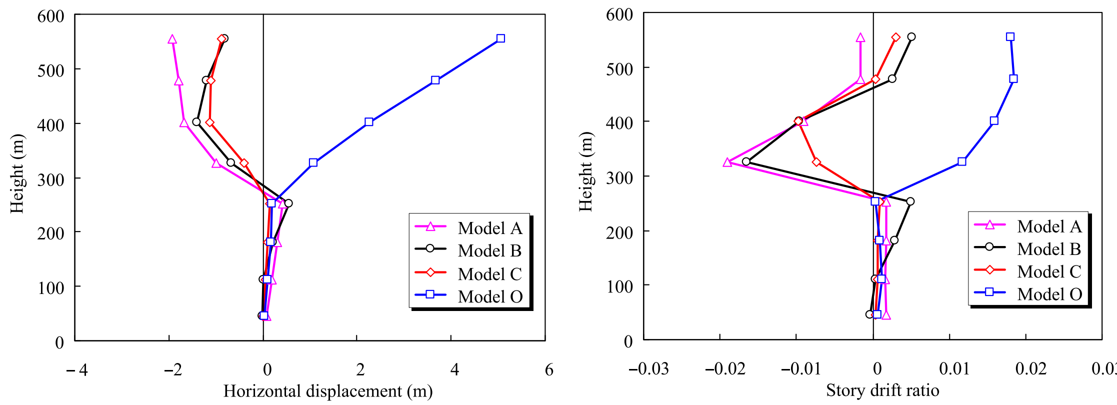

(a) Distribution of horizontal displacement. (b) Distribution of drift ratio in each zone.

Fig. 7. Distribution of the horizontal displacement along the height at the critical collapse state.

dimensionless parameter related to the correlation of the two modal shape vectors. The *NMD* is a close estimate of the average difference between the shape vectors of Models X and O. A smaller *NMD* value indicates a better correlation for the two modal shape vectors. Table 4 lists the values of *NMD* of Models A, B and C and Model O for the first three translational modes in both the *x* and *y* directions. A good correlation between the modal shapes of Models A, B and C and Model O is found, while a smaller stiffness of the soil–foundation system leads to a larger difference between the two modal shape vectors. On the whole, the SSI has a minor effect on the translational vibration modes of the Shanghai Tower.

3.2. Seismic collapse simulation considering the soil–structure interaction

Incremental dynamic analysis (IDA) (Vamvatsikos and Cornell, 2002) is an effective method to evaluate the seismic performance of structures and is widely used in structural seismic research. To evaluate the impact of the SSI on the collapse resistance of the Shanghai Tower, IDA is used to perform the collapse simulations of the four models. The commonly used ground motion recorded at the El-Centro station in USA in 1940 (referred to as “El-Centro” hereafter) is selected as a typical seismic input. The ground motion record is input along the *x* direction of the Shanghai Tower and the intensity increases gradually until collapse. During the collapse simulation, the classical Rayleigh damping is used with the 5% damping ratio specified in Section 5.3.4 of the Specification for the Design of Steel-Concrete Hybrid Structures in Tall Buildings (China Institute of Building Standard Design & Research, 2008).

The potential collapse process and failure mode of the Shanghai Tower without consideration of the SSI effect were predicted by Lu et al. (2011) to understand the earthquake-induced collapse mechanism subjected to extreme earthquakes. In comparison, this study focuses on the impact of the SSI on the collapse resistance of the Shanghai Tower; thus, the potential collapse process and the failure mode of Model B are discussed in detail in the following section, as an example to illustrate the SSI effect on the collapse resistance of the Shanghai Tower.

The earthquake-induced collapse is observed in Model B when the peak ground acceleration (*PGA*) of the El-Centro ground motion increases to 1.7*g* (*g* represents the gravity acceleration). The final collapse mode is shown in Fig. 5 and is mainly a vertical “pan-cake” collapse, similar to the description in Lu et al. (2011). The details of the collapse process are shown in Fig. 6. First, when t = 1.5 s (Fig. 6a), the diagonal members of the outriggers in Zones 4 and 5 begin to yield. When t = 2.6 s (Fig. 6b), some flange walls of the core tube at the bottom of Zone 7 are crushed as a result of the change of the openings layout in the core tube between Zones 6 and 7, which may lead to a sudden change in stiffness and a stress concentration. Next, when t = 3 s, the diagonal members of the outriggers in nearly all eight zones have undergone severe yield and begin to dissipate a large amount of seismic energy. Subsequently, when t = 3.43 s (Fig. 6c), the shear walls at the bottom of Zone 5 and the top of Zone 4 are crushed because the cross-section of the core tube is reduced from Zone 4 to Zone 5. When t = 3.58 s (Fig. 6d), some coupling beams along the *x* direction in the core tube begin to fail, and then the number of damaged coupling beams increases gradually. Later, when t = 5.38 s (Fig. 6e), most shear walls at the junction of Zones 4 and 5 have been damaged, and the vertical and horizontal loads distributed in the mega-columns increase gradually. Then, the mega-columns at the bottom of Zone 5 reach their ultimate capacities and begin to fail. Finally, when t = 6.28 s (Fig. 6f), the core tube and mega-columns at the bottom of Zone 5 are seriously damaged and unable to withstand the gravity and seismic loads. At this point, the entire structure begins to collapse.

The distribution of the horizontal displacement along the height of Model B at the critical collapse state in the *x* direction is shown in Fig. 7. At the critical collapse state, the deformation mode is similar to that in the third translational vibration mode, and the mass center of the building above the failure region does not exhibit a very significant horizontal displacement. Therefore, the failure of Model B is dominated by high-order vibration modes, and the main

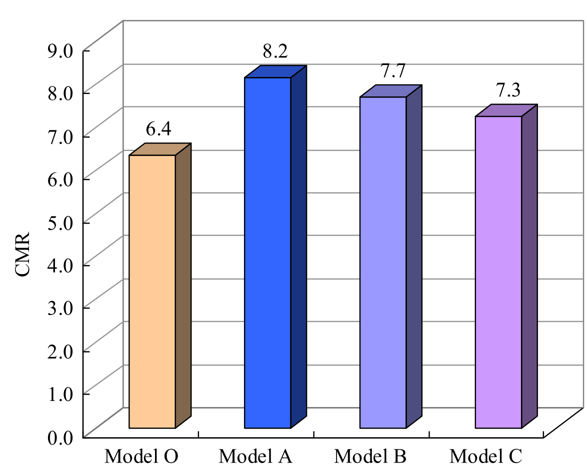

Fig. 8. Comparison of the CMR of the four models subjected to El-Centro in the *x* direction.

Table 5
Comparison of the failure sequences at the critical ground motion intensity of El-Centro.

Failure sequence	Model A	Model B	Model C	Model O
1	Diagonal members of the outriggers in Zones 4 and 5 begin to yield	Diagonal members of the outriggers in Zones 4 and 5 begin to yield	Diagonal members of the outriggers in Zones 4 and 5 begin to yield	Diagonal members of the outriggers in Zones 4 and 5 begin to yield
2	Shear walls at the bottom of Zone 7 begin to fail	Shear walls at the bottom of Zone 7 begin to fail	Shear walls at the junction of Zones 4 and 5 are crushed	Shear walls at the junction of Zones 4 and 5 are crushed
3	Shear walls at the junction of Zones 4 and 5 are crushed	Shear walls at the junction of Zones 4 and 5 are crushed	Coupling beams begin to fail	Some shear walls at the bottom of Zone 8 begin to fail
4	Coupling beams begin to fail	Coupling beams begin to fail	Mega-columns at the bottom of Zone 5 begin to fail	Coupling beams begin to fail
5	Mega-columns at the bottom of Zone 5 begin to fail	Mega-columns at the bottom of Zone 5 begin to fail	The entire structure begins to collapse	Mega-columns at the bottom of Zone 5 begin to fail
6	The entire structure begins to collapse	The entire structure begins to collapse		The entire structure begins to collapse

collapse mode of the Shanghai Tower is the vertical "pan-cake" collapse rather than lateral overturning.

3.3. *Comparison of the collapse resistance capacity and failure sequences*

In the IDA analysis, the ground motion intensity is increased gradually until the collapse occurs. Then, the critical ground motion intensity resulting in the structural collapse is obtained. In the study of structural seismic collapse prevention, the collapse margin ratio (CMR) is often used to quantify the capacity to resist structural collapse, which is calculated by the following equation, using *PGA* as the basic ground motion intensity measured in this research:

$$CMR = \frac{PGA_{\mathrm{Collapse}}}{PGA_{\mathrm{MCE}}} \tag{4}$$

where PGA_{Collapse} is the critical ground motion intensity resulting in the structural collapse, and PGA_{MCE} is the ground motion intensity corresponding to the maximum considered earthquake (MCE) level for the design. Shanghai is an Intensity 7 region and the corresponding PGA_{MCE} is 0.22*g*, as prescribed in the *Chinese Seismic Design Code* (GB50011-2010) (Ministry of Construction of the People's Republic of China, 2010).

With the El-Centro ground motion input in the *x* direction, Model O begins to collapse when the *PGA* is scaled to 1.4*g*; in comparison, the critical collapse *PGA*s of Models A, B and C are 1.8*g*, 1.7*g* and 1.6*g*, respectively. The CMR of these four models is compared in Fig. 8. It is clear that Model A has a maximum CMR of 8.2; the CMR of Model B is 7.7 and that of Model C is 7.3, while Model O has a minimum CMR of 6.4. The comparison shows that the consideration of the SSI effect increases the structural collapse resistance capacity. This increase is mainly because the SSI effect extends the vibrational periods of the Shanghai Tower and reduces the seismic demand of the structure under the same given ground motion records.

The failure sequences at the critical ground motion intensity of the four models subjected to El-Centro in the *x* direction are compared in Table 5. The entire failure sequences of these four models are very similar, i.e. the yield of the diagonal members of the outriggers in Zones 4 and 5 occurs first, followed by the crushing of the core tube, the failure of the coupling beam and the mega-columns at Zone 5, which is the main damaged region, and finally collapse occurs at the bottom of Zone 5, and the entire structure breaks into two parts. The difference is that the shear walls at the bottom of Zone 7 in Models A and B fail after the yielding of diagonal members of the outriggers in Zones 4 and 5; however, no failure of the shear wall in Zone 7 is observed in Model C in the early stage of collapse simulation, and in Model O, some shear walls at the bottom of Zone 8 are crushed instead of at Zone 7. The distributions of the horizontal displacements along the height at the critical collapse state and the time-histories of the roof vertical displacements of the four models are shown in Figs. 7 and 9, respectively. In Models A, B and C, the deformation mode at the critical collapse state is similar to that in the high-order vibration mode. The mass center of the structure above the failure region does not undergo a very significant displacement, and the final collapse mode is the vertical "pan-cake" collapse. In Model O, the collapse occurs at $t = 20.23$ s when Model O has entered the stage of free vibration. Because severe damage has occurred in the structure due to the earthquake, the development of structural damage continues after entering the free vibration stage, and finally the entire structure breaks into two parts at the bottom of Zone 5. Therefore, the deformation mode at the critical collapse state of the structure above the failure region is very similar to that in the first vibration mode; however, the final collapse mode is still the vertical "pan-cake" collapse.

4. Conclusions

In this study, the substructure approach is used to evaluate the influence of the SSI on the seismic collapse resistance of the Shanghai Tower. The refined FE model of the superstructure of the Shanghai Tower and the simplified analytical model of the foundation and adjacent soil are established to predict the collapse process and collapse mode while considering the SSI, as well as the influence of the SSI on the capacity to resist collapse and failure sequences. The following conclusions are drawn:

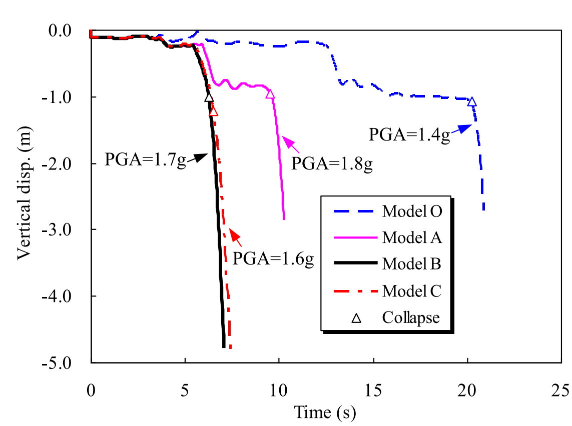

Fig. 9. Roof vertical displacement time-histories at the critical ground motion intensity of El-Centro.

(1) The SSI effect could extend the periods of lower order vibration modes, particularly the fundamental period, and a smaller stiffness of the soil–foundation system leads to longer vibration periods. However, the SSI effect has a minor influence on the translational vibration modal shape vectors of the Shanghai Tower.
(2) The SSI effect improves the collapse resistance capacity of the Shanghai Tower, and a smaller stiffness of soil–foundation system leads to a larger CMR.
(3) The SSI effect has some impact on the failure sequences of the Shanghai Tower subjected to extremely strong earthquakes but a negligible impact on the final failure modes.

Conflict of interest

We wish to confirm that there are no known conflicts of interest associated with this publication and there has been no significant financial support for this work that could have influenced its outcome.

Acknowledgments

The authors are grateful for the financial support received from the National Nature Science Foundation of China (Nos. 51222804, 91315301), the Beijing Natural Science Foundation (No. 8142024) and the Fok Ying Dong Education Foundation (No. 131071).

References

ATC. Soil-structure interaction for building structures (ATC 84). Redwood City, California: Applied Technology Council; 2012.
Avilés J, Pérez-Rocha LE. Soil-structure interaction in yielding systems. Earthquake Engineering and Structural Dynamics 2003;32(11):1749–71.
Banerjee S, Lee FH. Centrifuge shaking table tests on a single pile embedded in clay subjected to earthquake excitation. International Journal of Geotechnical Engineering 2013;7(2):117–23.
Chaallal O, Ghlamallah N. Seismic response of flexibly supported coupled shear walls. Journal of Structural Engineering 1996;122(10):1187–97.
Chang BJ, Raychowdhury P, Hutchinson TC, Thomas JM, Gajan S, Kutter BL. Evaluation of the seismic performance of combined frame-wall-foundation structural systems through centrifuge testing. In: Proceedings of the 4th international conference on earthquake geotechnical engineering. Thessaloniki, Greece: Springer; 2007. Paper No. 1497.
Chen WH, Lu ZR, Chen SH, Ni YQ, Liao WY. Monitoring dynamic characteristics of Canton Tower under different excitations. Journal of Vibration and Shock 2012;32(3):49–54 (in Chinese).
China Institute of Building Standard Design & Research. Specification for design of steel-concrete mixed structure of tall buildings (CECS 230: 2008). Beijing: China Planning Press; 2008 (in Chinese).
Ciampoli M, Pinto PE. Effects of soil-structure interaction on inelastic seismic response of bridge piers. Journal of Structural Engineering 1995;121(5):806–14.
Deng L, Kutter BL, Kunnath S. Centrifuge modeling of bridge systems designed for rocking foundations. ASCE Journal of Geotechnical and Geoenvironmental Engineering 2012;138(3):335–44.
Drosos V, Georgarakos T, Loli M, Anastasopoulos I, Zarzouras O, Gazetas G. Soil-foundation-structure interaction with mobilization of bearing capacity: an experimental study on sand. ASCE Journal of Geotechnical and Geoenvironmental Engineering 2012;138(11):1369–86.
Farghaly AA, Ahmed HH. Contribution of soil-structure interaction to seismic response of buildings. KSCE Journal of Civil Engineering 2013;17(5):959–71.
Gao XW, Bu QS. Rational factor of cycle reduction and inter-story elastic drift correction for multi-story RC-frame building. Building Structure 1993;17(2):42–6 (in Chinese).
Gazetas G, Mylonakis G. Seismic soil-structure interaction: new evidence and emerging issues. In: Geotechnical earthquake engineering and soil dynamics III, vol. 2. Reston, Virginia: American Society of Civil Engineers; 1998. pp. 1119–74.
Han Y. Seismic response of tall building considering soil-pile-structure interaction. Earthquake Engineering and Engineering Vibration 2002;1(1):57–64.
Jarernprasert S, Bazan-Zurita E, Bielak J. Seismic soil-structure interaction response of inelastic structures. Soil Dynamics and Earthquake Engineering 2013;47:132–43.
Jiang XL, Li BQ, Lao HY. Seismic response analysis of pile-soil-structure of the Shanghai Tower's Miranda model. Earthquake Resistant Engineering and Retrofitting 2013;35(4):42–7 (in Chinese).
Li WY. China: a country locked in fierce competition to build super high-rises. Time Architecture 2011;28(3):9 (in Chinese).
Li ZQ. Research on structure health monitoring of Jin Mao Tower [Ph.D. Thesis]. Shanghai: Tongji University; 2007 (in Chinese).
Liu W, Hutchinson TC, Kutter BL, Hakhamaneshi M, Aschheim M, Kunnath S. Demonstration of compatible yielding between soil-foundation and superstructure components. Journal of Structural Engineering, ASCE 2012;139:1408–20.
Lu XL, Chen YQ, Chen B, Huang W, Zhao L. Shaking table testing of dynamic soil-structure interaction system. Journal of Earthquake Engineering and Engineering Vibration 2000;20(4):20–9 (in Chinese).
Lu XL, Li PZ, Guo XQ, Shi WX, Liu J. Vibration control and site measurement on Shanghai World Financial Center Tower. Structural Engineers 2009;25(4):63–70 (in Chinese).
Lu XL, Shi WX, Shen JH, Fan PF. Measurement on dynamic property of several super high-rise buildings in Shanghai. Building Science 2001;17(2):36–9 (in Chinese).
Lu XL, Chen B, Li PZ, Chen YQ. Numerical analysis of tall buildings considering dynamic soil-structure interaction. Journal of Asian Architecture and Building Engineering 2003;2(1):1–8.
Lu X, Lu XZ, Zhang WK, Ye LP. Collapse simulation of a super high-rise building subjected to extremely strong earthquakes. Science China Technological Sciences 2011;54(10):2549–60.
Luco JE, Trifunac MD, Wong HL. Isolation of soil-structure interaction effects by full-scale forced vibration tests. Earthquake Engineering and Structural Dynamics 1988;16(1):1–21.
Meyerhof GG. Some recent foundation research and its application to design. Structural Engineer 1953;31(6):151–67.
Ministry of Construction of the People's Republic of China. Code for seismic design of buildings (GB50011-2010). Beijing: China Architecture and Building Press; 2010 (in Chinese).
Mylonakis G, Gazetas G. Seismic soil-structure interaction: beneficial or detrimental? Journal of Earthquake Engineering 2000;4(3):277–301.
Mylonakis G, Syngros C, Gazetas G, Tazoh T. The role of soil in the collapse of 18 piers of Hanshin Expressway in the Kobe earthquake. Earthquake Engineering and Structural Dynamics 2006;35(5):547–75.
Pitilakis D, Clouteau D. Equivalent linear substructure approximation of soil-foundation-structure interaction: model presentation and validation. Bulletin of Earthquake Engineering 2010;8(2):257–82.
Ravichandran N, Krishnapillai S, Machmer B. Centrifuge modeling of unsaturated soil-pile system. In: Proceedings of GeoCongress 2012: state of the art and practice in geotechnical engineering. Oakland, California: American Society of Civil Engineers; 2012. pp. 1978–87.
Stewart JP, Fenves GL, Seed RB. Seismic soil-structure interaction in buildings. I: analytical methods. Journal of Geotechnical and Geoenvironmental Engineering 1999;125(1):26–37.
Vamvatsikos D, Cornell CA. Incremental dynamic analysis. Earthquake Engineering and Structural Dynamics 2002;31(3):491–514.
Veletsos AS, Meek JW. Dynamic behaviour of building-foundation systems. Earthquake Engineering and Structural Dynamics 1974;3(2):121–38.
Wang MW. Dynamic centrifuge tests and numerical modelling for geotechnical earthquake engineering in liquefiable soils. Beijing: Science Press; 2012 (in Chinese).
Wang XL, Qu WL, Liu H. Finite element analysis on dynamic characteristics of super high tower in Guangzhou. Journal of Wuhan University of Technology 2007;29(1):142–4 (in Chinese).
Waters TP. Finite element model updating using measured frequency response functions [Ph.D. Thesis]. Bristol: University of Bristol; 1995.
Wolf JP. Dynamic soil-structure interaction. Englewood Cliffs, N.J.: Prentice-Hall, Inc.; 1985.
Zhu JJ, Lu XL, Zou Y. Shake-table test and theoretical analysis for Shanghai World Financial Center scale model. China Civil Engineering Journal 2005;38(10):22–30 (in Chinese).
Zhu JJ, Lu XL. Elastoplastic time-history analysis of Shanghai World Financial Center building. Journal of Natural Disasters 2006;15(2):49–56 (in Chinese).

Mengke Li is now a postgraduate student of Department of Civil Engineering, Tsinghua University, Beijing. She is engaged in performance-based seismic design and evaluation for high-rise buildings.